Desalination and Water Treatment
www.deswater.com

doi: 10.1080/19443994.2015.1072743

57 (2016) 15410–15423
July

Taylor & Francis
Taylor & Francis Group

Response surface modeling of Cu(II) removal from wastewater using fish scale-derived hydroxyapatite: application of Box–Behnken experimental design

N. Mandal[a], S. Mondal[a], A. Mondal[b], K. Mukherjee[a], B. Mondal[a,*]

[a]*Centre for Advanced Materials Processing, CSIR-Central Mechanical Engineering Research Institute (CSIR-CMERI), Mahatma Gandhi Avenue, Durgapur 713 209, India, Tel. +91 9932399947; email: n_mandal@cmeri.res.in (N. Mandal), Tel. +91 9851265212; email: mailsudipmondal@gmail.com (S. Mondal), Tel. +91 9775552143; email: kalisadhanm@yahoo.com (K. Mukherjee), Tel. +91 9434333054, +0343 6510218; Fax: +91 343 2546745; emails: bnmondal@rediffmail.com, bnmondal@cmeri.res.in (B. Mondal)*

[b]*Department of Biotechnology, National Institute of Technology, Durgapur Mahatma Gandhi Avenue, Durgapur 713 209, India, Tel. +91 9674006999; email: arn.spark9@gmail.com*

Received 24 December 2014; Accepted 8 July 2015

ABSTRACT

The present study illustrates the potential use of hydroxyapatite (HAp) synthesized from fish scale for Cu(II) removal with optimal efficiency. Batch experiments were conducted to determine the effects of varying parameters like contact time (40–200 min), initial metal ion concentration (100–300 mg/L), and pH (2–9). The adsorption kinetics was investigated using pseudo-first-order and pseudo-second-order kinetics. The Langmuir and Freundlich isotherm equations have been also studied for the equilibrium modeling of adsorption systems. The maximum adsorption capacity of fish scale-derived HAp on copper removal is found to be 209.732 mg/g. Box–Behnken design of response surface methodology with three variables was carried out to establish a significant correlation between the effects of these parameters to the amount of Cu(II) adsorbed. The initial Cu(II) concentration 212.93 mg/L, pH 8, and contact time 40 min are also found to be optimum for sorption of Cu(II) onto *Labeo rohita* scale-derived HAp with removal efficiency of 91.77%.

Keywords: Adsorption; Copper(II); Hydroxyapatite; *Labeo rohita* scale; Optimization

1. Introduction

In recent years, water pollution due to the disposal of heavy metals has been an increasing global environmental concern. Heavy metals in the environment creates a problem due to their increasing discharge, toxic nature, and other adverse harmful effects (carcinogenic, mutagenic, or bioaccumulation) on animal and plant biota [1]. The major industrial sources of heavy metals which contaminate the water bodies are mainly leather and tanning, electroplating, paper industry, batteries, metal smelting, metal mining, petrochemical, plastics, electronics, and textile dye industries. The harmful heavy metals such as copper, cobalt, silver, zinc, lead, cadmium, aluminum, chromium, iron, nickel, and mercury are frequently discharged from those industries into the water stream which adversely affects the environmental system [2].

---

*Corresponding author.

The heavy metals are known to be stable and persistent environmental contaminants since they cannot be degraded or destroyed. Copper (Cu), one of the hazardous heavy metals, finds its way to water bodies through wastewater from different industries like copper wire mills, coal burning industries, tanning, alloy industries, metal cleaning, and plating baths [3]. High concentration of copper causes neurotoxicity commonly known as "Wilson's disease." The other effects of copper include congestion of nasal mucous membranes and pharynx, ulceration of nasal septum, and metal fume fever [4].

The conventional wastewater treatments which used for heavy metal ions removal are including adsorption, chemical precipitation, electrolysis, reverse osmosis, ion exchange, and membrane filtration. Among all these processes, adsorption has been suggested as being less expensive, easy to handle, and effective method for heavy metal removal [5]. The development of new low-cost eco-friendly sorbents such as red mud and fly ash, sawdust, tea industry waste, magnetite, hydroxyapatite (HAp), olive cake, and rice husk has therefore become relevant recently for removal of toxic heavy metals [6–8]. Nowadays, the increasing interests of removing metal ions from the wastewater motivates the researchers to try different adsorbing materials like cement, gypsum, lime, coal, bentonite, clay, agricultural waste, biomass, tree leaves, microbes, and fungus [9–11].

Most of these experimental works will be highly influenced by several variables like pH, sorbent concentration, temperature, and time of contact for better adsorption efficiency. Working with this variable parameter is extremely time consuming, expensive, and difficult to culminate the best condition for adsorption. To overcome this difficulty with large number of variables, experimental Box–Behnken design under response surface methodology (RSM) has been employed to optimize the adsorptions of heavy metals [12]. Different studies have been employed by researchers to remove heavy metals like cadmium, nickel, and lead using fungus [13,14] chromium by biomass [15,16], silver by tree leaves [17–20], copper by raw, and calcined phosphogypsum, rice husk, grafted silica, sawdust, wheat straw, and tree leaves [21–27]. Different adsorbents (from literature) along with their adsorption capacities for copper ions has been presented in Table 1 [28–39]. But, no investigation has been carried so far for optimizing copper adsorption using HAp powder obtained from fish scale and visualizes the effect of parameters which control the adsorption process using RSM.

The present investigation is aimed at exploring combined effect of various process parameters like Cu(II) concentration, pH of the solution, and contact time on removal of Cu(II) from aqueous solution by HAp using Box–Behnken experimental design. Subsequently, the optimization of the metal removal percentage with respect to different parameters is also carried out. Synthetic HAp was used by several researchers for removal of heavy metal ions.

Choice of HAp as sorbent is based on the fact that it is abundant, stable under reducing condition, nontoxic, and can be synthesized in low-cost environment friendly manner [40]. The present study illustrates possible use of HAp synthesized from natural resources like fish scale as an adsorbent for removal of Cu(II) from aqueous solution by batch experimentation. The RSM, which is a combination of mathematical and statistical techniques, has been used for optimizing the processes and to evaluate the relative significance of several process parameters [41]. In the present case, Box–Behnken model experimental design in RSM by Design Expert Version 6.0.10 (Stat Ease, USA) is applied to analyze the efficiency of the system under different conditions. Box–Behnken is a spherical revolving design which requires an experiment number according to $N = k^2 + k + \mathrm{cp}$ where k is the factor number and cp is the replicate number of central point [42]. The present work is aimed at finding combined effect of various process parameters like Cu(II) concentration, pH of the solution, and duration of removal of Cu(II) from aqueous solution by *Labeo rohita*-derived HAp ceramic using Box–Behnken experimental design. The optimized condition of process parameters for maximum Cu(II) removal is revealed in the present study.

2. Materials and methods

2.1. Synthesis and characterization of HAp powder

Fish scales are collected from freshwater fish (*L. rohita*) and initially deproteinized through external washing with 1 (N) HCl (Merck, 35%) solution (2:1, v/w, water HCl/fish scale) for 24 h at room temperature (28 ± 2˚C) followed by acetic acid treatment for the removal of collagen fibers. The filtered fish scales are washed thoroughly with distilled water and dried at 60˚C in hot air oven for several hours. Treated fish scales are calcined at 1,200˚C to synthesize HAp bio-ceramics.

The crystalline phase and different functional groups of synthesized powder are analyzed by X-ray diffraction studies (International Centre for Diffraction Data using the cards 00-009-0432) and Fourier transform infrared (FTIR) spectroscopy. Morphology of the HAp powder before and after adsorption is observed

Table 1
Different adsorbents along with their adsorption capacities for copper ions

Sl. No.	Adsorbent	Cu(II) solute conc. $Q_{\max}$	Refs.
1	Natural iron oxide-coated sand	2.040	[28]
2	Modified mangrove bark	6.950	[29]
3	Black carrot (*Daucus carota* L.) residues	8.745	[30]
4	Mushroom (*Agaricus bisporus*)	9.116	[31]
5	Chitosan/clinoptilolite composite	11.320	[32]
6	Papaya wood	19.9	[33]
7	Peanut hull	21.25	[34]
8	Rice bran	27.81	[35]
9	Sugar beet pulp	31.4	[36]
10	Fish scale	58.5	[37]
11	Garlic skin	76.3	[38]
12	Onion skin	80.6	[38]
13	Activated carbon,	125.0	[39]
14	Fly ash	181.8	[39]
15	Fish scale HAp	209.732	In this study
16	Sissoo sawdust	263.2	[39]

by scanning electron microscopy (SEM) and high-resolution transmission electron microscopy (TEM, JEOL Model JEM 2010).

2.2. Batch studies

The batch adsorption experiments are conducted with HAp at room temperature in 250-ml Erlenmeyer flasks on thermostatic orbital shaker at 180 rpm. At specific time interval, samples are separated by centrifugation at constant intervals. The % removal of Cu(II) is calculated using Eq. (1):

$$\%\,\text{Removal} = (C_0 - C_e) \times 100/C_0 \tag{1}$$

where C_0 and C_e are initial and final metal ion concentrations (mg/L).

The Cu^{2+} adsorption capacity of HAp is calculated using Eq. (2).

$$q = (C_0 - C_e) \times V/M \tag{2}$$

where C_0 and C_e are defined above, q (mg/g) is the adsorption capacity per unit of HAp, M (g) is the mass of HAp, and V (L) is the volume of sample taken.

At the end of the adsorption process, adsorbent is separated from the solution and supernatant is analyzed for residual Cu(II) concentration by AAS (Perkin–Elmer 700).

The effect of pH on the adsorption capacity is investigated at pH values in the range of 2.0–9.0 using known volume of 200 mg/L Cu(II) solutions. The desired pH of the solutions is maintained by adding HCl or NaOH at the beginning of the experiment. The effect of contact time is studied in the time range of 20–180 min. Elute is collected after 10-min interval and analyzed by AAS to determine the removal percentage.

Cu(II) solutions with initial concentration of 50, 100, 200, and 300 mg/L are equilibrated with HAp to determine the possible effect of metal ion concentration during adsorption process. The batch experimentation is carried out using fish scale-derived HAp as an adsorbent.

Kinetic measurements are conducted under static conditions employing a glass vessel equipped with a rotary shaker. Thus, the adsorbent dose of 2 g of HAp is contacted with 100 ml of a Cu(II) ion solution of known concentrations varying from 50 to 300 mg/L. The concentration of Cu(II) ion in the wastewater is determined at known time intervals.

2.3 Optimization of sorption process using RSM approach

Box–Behnken model for three variables (metal concentration, pH, and contact time), each with two levels (the minimum and the maximum), is used as experimental design model. The model has the advantage that it permits the use of relatively few combinations of variables for determining the complex response function. A total of 17 experiments are required to be performed to calculate 10 coefficients of second-order polynomial equation [43]. In this experimental design model, optimization is carried out by choosing three independent process variables viz., metal ion concentration (100–300 mg/L), pH (2–8), and contact time (40–140 min). These are taken as input variables. Percent removal of Cu(II) from the solution is taken as response of the system.

Percent copper removal by HAp in different experimental conditions based on the experimental design matrix is estimated and the results are reported in experimental design section. A second-order polynomial model where interaction terms have been fitted to the experimental data obtained from the Box–Behnken model experiment can be stated in the form of the following equation:

$$Y = A_0 + \sum A_{\mathrm{i}} X_{\mathrm{i}} + \sum A_{\mathrm{ii}} X_i^2 + \sum A_{\mathrm{ij}} X_{\mathrm{i}} X_{\mathrm{j}} \quad (3)$$

where Y is the percentage of metal adsorbed, A_0 is the offset term, A_{i} the first-order main effect, A_{ii} is the second-order main effect, and A_{ij} is the interaction effect. The data are subjected to analysis of variance and the coefficient of regression (R^2) is calculated to find out the goodness of fit of the model. The desirability function optimization of the RSM has been employed for single response optimization. The optimization module searches for a combination of factor levels that simultaneously satisfies the requirements placed on each of the responses and factors in an attempt to establish the appropriate model.

3. Results and discussion

3.1. Characterization of sorbent

Fig. 1 shows XRD pattern of synthesized powder HAp as the only phase. Well-resolved characteristic peak of highest intensity for HAp is obtained at 2θ value of 31.77° corresponding to 211 plane. Sharp peak intensity and well-resolved peaks in XRD patterns prove complete crystallization of the powder.

The FTIR spectrum shows all characteristic absorption peaks of HAp as depicted in Fig. 2. The first indication for formation of HAp is in the form of a strong complex broad FTIR band centered at about 1,000–1,100 cm^{-1} due to asymmetric stretching mode of vibration for PO_4 group. The band at 576.30 cm^{-1} corresponds to n4 symmetric P–O stretching vibration of the PO_4 group [44–47]. The band at 2,005–2,079 cm^{-1} is due to overtone of 1,040 cm^{-1} band. The crystalline powder generates two characteristic stretching modes of O–H bands at about 3,571.23 and 462 cm^{-1} which are noticed in FTIR spectrum. The morphology of the fish scales have been studied and reported in Fig. 3. Initially, fish scales washed with diluted 1 (N) HCl (Merck, 35%) shows that the collagen fibers are well interconnected on the scale surface as revealed in Fig. 3(a). Further, this interconnected collagen fibers can be removed with acetic acid (0.5 M) solution to obtain collagen free scale for organic impurities free HAp preparation. The SEM micrographs of HAp powder without or with adsorption of Cu(II) are shown in Fig. 3(b) and (c), respectively. The synthesized HAp powder is soft granule ultrafine particle and demonstrates a very good homogeneity of the powder surfaces. After Cu(II) adsorption onto HAp in needle shape is depicted in Fig. 3(c). It is also further revealed from TEM images that the needle shape morphology, mostly agglomerated as

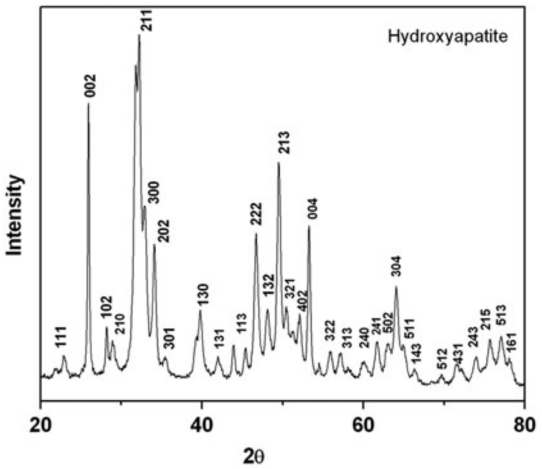

Fig. 1. XRD pattern of HAp powder synthesized from fish scale.

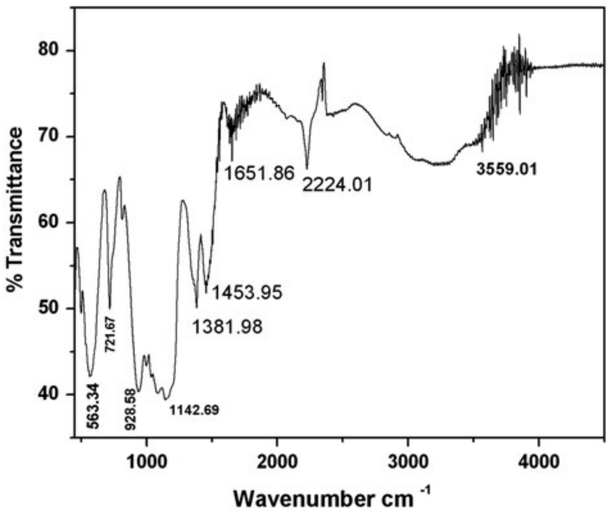

Fig. 2. FTIR spectrum of HAp powder synthesized from fish scale.

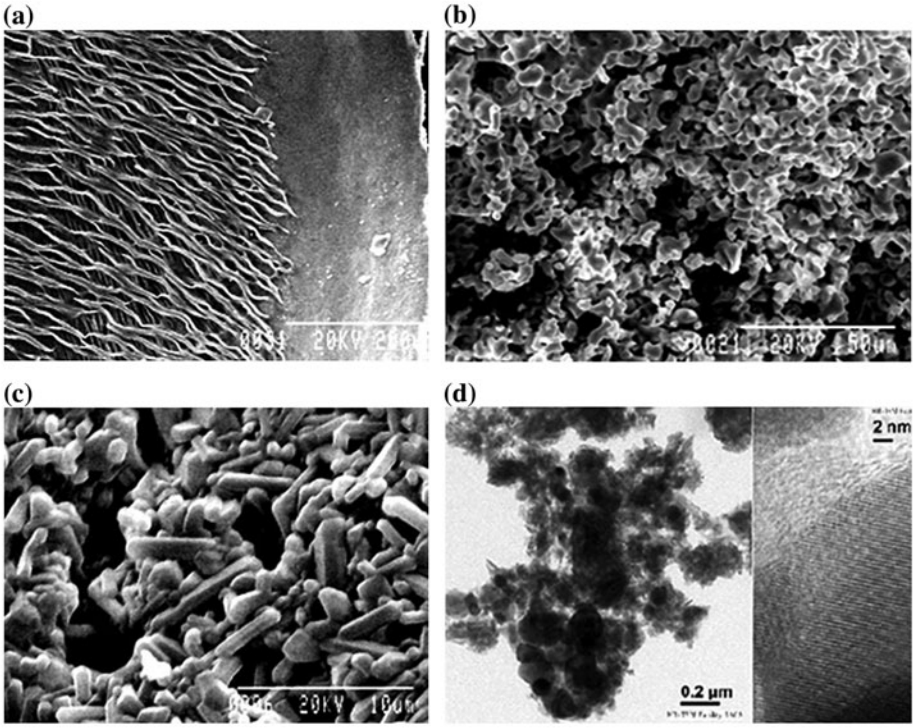

Fig. 3. SEM images of (a) interconnecting collagen fibers on fish scale surface (b) synthesized HAp from fish scale before adsorption (c) HAp after adsorption of Cu(II), and (d) TEM images of synthesized HAp.

depicted in Fig. 3(d), is attributed to adsorption of Cu(II). The particle size in length is in the order of 25–50 nm and width of 10–17 nm.

4. Sorption study

Fig. 4 shows the batch experiments regarding the sorption capacity of Cu(II) ions by HAp, i.e. q (mg/g) as a function of contact time t (min). Aqueous solutions of different initial concentrations (50, 100, 200, and 300 mg/L) of Cu(II) with pH 6.0 have been considered for the study. The selection of pH 6.0 is based on our experimental results (adsorption % vs. pH) as shown in Fig. 4 (inset). The effect of pH for adsorption of Cu(II) on HAp has been studied by varying pH in the range of 2–9 using copper contaminated water with initial concentration of 200 mg/L. It has been observed that adsorption % of metal ions increases with increment of pH from 2 to 6 and reaches equilibrium at pH 6–8. Above pH 8, there is a little decrease in adsorption due to the precipitation of Cu(II) at high pH. From Fig. 4, it is clearly seen that equilibrium between Cu^{2+} and HAp is attained within 140 min since there is no significant change after that. The maximum removal occurs in first 60 min, and then subsequently slow removal occurs until equilibrium is reached.

As shown in Fig. 4, the sorption capacity q (mg/g) of Cu^{2+} ion is increased by increasing initial metal ion concentration. Higher initial concentration is an important driving force to overcome all mass transfer resistance of pollutant between the aqueous and solid phases, thus increased the uptake.

4.1. Kinetics study

To study kinetics of the adsorption process of two different kinetic models, i.e. pseudo-first-order, pseudo-second-order kinetic models are tested on experimental data.

The simplified pseudo-first-order equation is expressed [48] as

$$\log(q_e - q_t) = \log(q_e) - (k_1 t)/2.303 \tag{4}$$

where q_e and q_t are the adsorption capacity at equilibrium and at time t, respectively (mg/g) and k_1 is the rate constant of pseudo-first-order adsorption (l/min). A plot of log $(q_e - q_t)$ vs. t should give a straight line, if the sorption is controlled by this model. k_1 and q_e

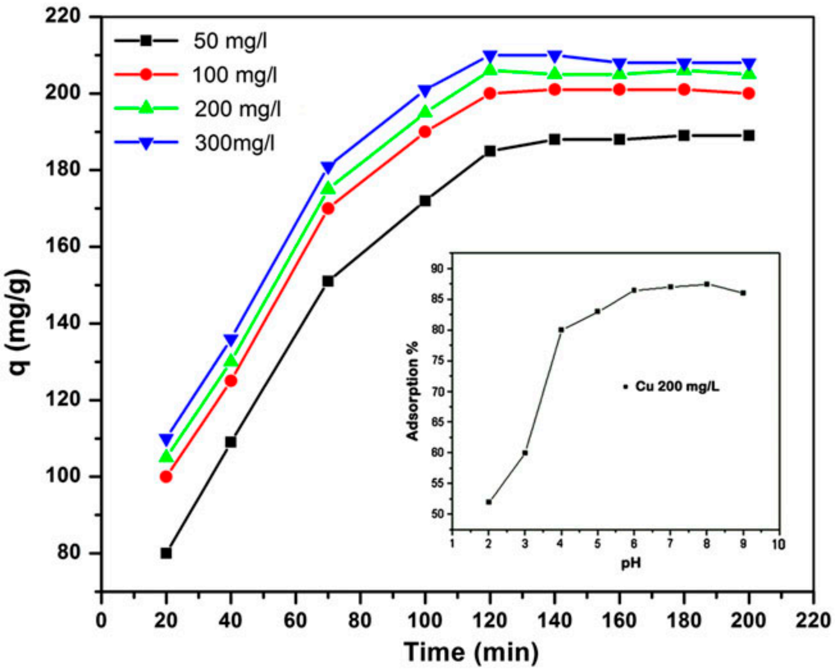

Fig. 4. Effect of contact time on sorption capacity of Cu(II) onto HAp (inset: adsorption % vs. pH).

can be determined from the slope and intercept of the plot, respectively.

The simplified form of pseudo-second-order adsorption can be presented as follows:

$$t/q_t = 1/k_2 q_e^2 + (1/q_e)t \tag{5}$$

where q_t is the amount of metal ions adsorbed (mg/g) at any given time t (min), q_e is the amount of metal ion adsorbed (mg/g) at equilibrium, and k_2 is the second-order reaction rate constant for adsorption [mg (g/min)].

Fig. 5 shows the plot of pseudo-first-order (Fig. 5 inset one) and pseudo-second-order model for Cu^{2+} adsorption on HAp, respectively. In this kinetic study, reaction constants, R^2 values, and experimental q_e values of pseudo-first- and second-order kinetics have been presented by Table 2. From this table, the average correlation coefficient values of R^2 have been calculated for the pseudo-first-order kinetic model which is 0.966 and for pseudo-second-order model which is 0.999. It is clear from R^2 values that the adsorption process follows pseudo-second-order kinetic model better than first-order kinetic model.

This suggests that the rate-limiting step of this sorption system may be chemical sorption or chemisorptions involving valence forces through sharing or exchange of electrons between sorbent and sorbet [49,50]. The experimental q_e is found to be close to the estimated one and increases with increase in Cu(II) concentration. k_2 values are decreased with increase in initial Cu^{2+} concentration which suggests increased adsorption [51].

4.2. Sorption isotherm

Langmuir and Freundlich isotherm [52] equations have been used to study the equilibrium modeling of adsorption systems. The equilibrium data for metal ions are studied over concentration range of 50–350 mg/L at room temperature.

Freundlich isotherm can be expressed as follows in linear form:

$$\ln q_e = \ln K_f + 1/n \ln C_e \tag{6}$$

Fig. 6 shows fitting plot of Langmuir isotherm (C_e/q_e vs C_e) where q_e (mg/g) is the amount of metal ion adsorbed at equilibrium per g of adsorbent, C_e (mg/L) is the equilibrium concentration of metal ion in the solution; K_f and n are the Freundlich model constants [53,54]. Freundlich isotherm is used to describe surface heterogeneity and the exponential distribution of active sites and energies. Fig. 6 inset shows the fitting plot of Freundlich isotherm ($\ln Q_e$ vs $\ln C_e$) of Cu^{2+} ions onto HAp.

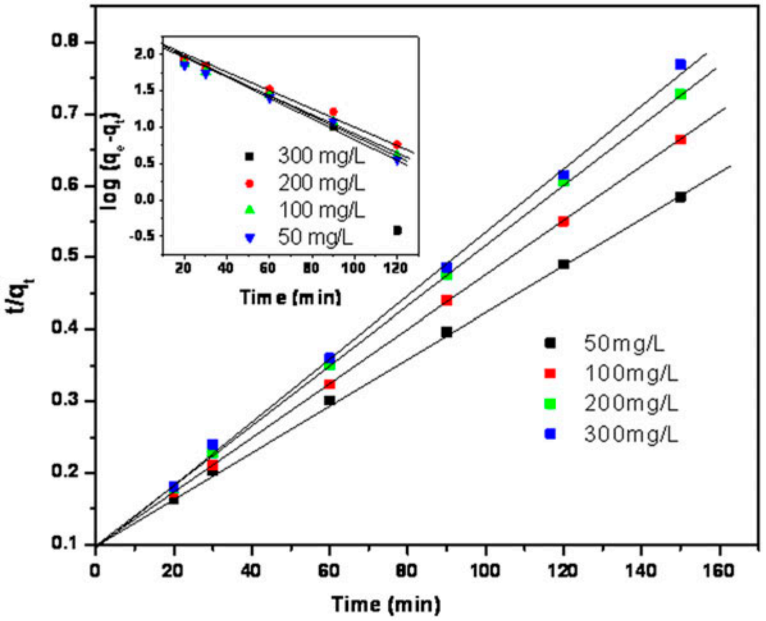

Fig. 5. Pseudo-second-order kinetic model of Cu^{2+} adsorption onto HAp at room temperature (inset: pseudo-first-order kinetic model).

Table 2
Reaction constants, R^2 values, and experimental q_e values of pseudo-first- and second-order kinetics

		Cu(II) concentration (mg/L)				
Kinetic model	Parameter	50	100	200	300	Average
Pseudo-first-order	K_1 (min^{-1})	0.0481	0.0276	0.253	0.021	
	q_e (mg/g)	135.5	139.31	155.2	253.8	
	R^2	0.988	0.994	0.993	0.892	0.966
Pseudo-second-order	K_2 (g/mg/min)	0.00024	0.00012	0.00011	0.00011	
	q_e (mg/g)	200	250	252	255	
	R^2	0.999	0.999	0.998	0.999	0.999

The maximum sorption capacity (K_f) found 145.4 mg/g with affinity value (n) equal to 11.8.

Linear form of Langmuir equation can be expressed as follows

$$C_e/q_e = 1/X_m K + (1/X_m)C_e \tag{7}$$

where q_e (mg/g) is the amount adsorbed at equilibrium onto HAp, C_e (mg/L) is the equilibrium concentration of metal in solution, X_m (mg/g) is the maximum sorption capacity, and K (L/mg) is the Langmuir constant related to energy of adsorption [52]. A linear plot of Langmuir isotherm with experimental data is obtained when C_e/Q_e is plotted against C_e over entire range of Cu^{2+} ion concentration. The adsorption constants of Langmuir and Freundlich equation and their correlation coefficients (R^2) are calculated and shown in Table 3

It is clear from R^2 value that Langmuir isotherm is fitted better over Freundlich isotherm for Cu^{2+} adsorption on HAp. The maximum sorption capacity (X_m) calculated for Langmuir equation was 209.732 mg/g. Maximum sorption capacity from Langmuir equation represents the monolayer coverage of sorbent with sorbet.

4.3. Response surface methodological approach

4.3.1. RSM evaluation

When fitting the model, various statistical analysis techniques are employed to judge the experimental

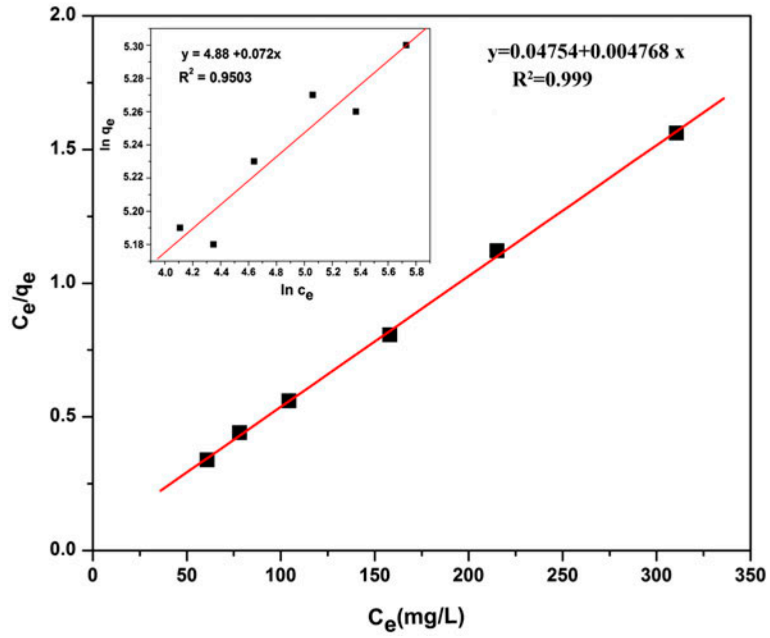

Fig. 6. Linear fit of Langmuir isotherm plot (inset: Freundlich isotherm plot) for adsorption of Cu^{2+} onto HAp.

Table 3
Adsorption constants of Langmuir and Freundlich equations and their correlation coefficients R^2

	Langmuir			Freundlich		
Metal ion	X_{max}	K	R^2	K_f	n	R^2
Cu(II)	209.732	0.1003	0.999	145.4	11.8	0.95

error, the suitability of model, and statistical significance of the terms in model. This is usually done using either a statistical package or a RSM program. Some of the model items may turn out to be insignificant for a good representation of experimental data so usually a subset of model with fewer terms is selected. There are often several subsets that lead to similar results, so care must be taken when trying to interpret single model term. The final model can be used to create graphical representations of parameter dependencies, e.g. as contour plots to see the relative influence of parameters to find optimum parameter combination and to predict experimental results for other parameter combinations [55,56].

4.3.2. Experimental design

The quadratic equation model for predicting the optimal point was stated according to Eq. (3). The optimum values of the selected variables are obtained by solving the regression equation and by analyzing the response surface contour plots. The results of each experiment performed as per the software are given in Table 4.

An empirical relationship between the response and the independent variables has been expressed by the following quadratic model. The following equations are the final empirical models in terms of coded factors for:

$$Y = 71.25 + 15.28A - 2.41B + 6.27 \times C + 3.13AB - 3.94AC + 7.522A^2 - 2.88B^2 \quad (8)$$

While the following equations are the final empirical model in terms of actual factor for:

$$\begin{aligned}\%\ \text{Removal} = {} & 47.29 - 2.99\ \text{pH} + 0.04\ \text{Concentration} \\ & + 0.26\ \text{Time} + 0.01\ \text{pH Concentration} \\ & - 0.03\ \text{pH time} + 0.83\ \text{pH}^2 - 2.88 \\ & \times 10^{-4}\ \text{Concentration}^2\end{aligned} \quad (9)$$

4.3.3. Analysis of variance

The adequacy and significance of the regression model is tested using ANOVA method. Test for significance on individual model coefficients and test for lack-of-fit is also estimated. An ANOVA table is commonly used to summarize the test performed. The

Table 4
Experimental result as per Box–Behnken design matrix

Experimental run	pH	Concentration (mg/L)	Time (mins)	Removal %
1	5	200	90	71.85
2	8	300	90	92.92
3	5	300	140	73.286
4	2	200	40	53.911
5	5	100	40	65.286
6	5	200	90	71.85
7	5	200	90	70.95
8	2	100	90	65.65
9	5	100	140	77.51
10	8	200	140	95.221
11	5	300	40	56.318
12	5	200	90	72.26
13	2	300	90	56.35
14	8	100	90	89.684
15	8	200	40	92.62
16	2	200	140	72.278
17	5	200	90	70.389

insignificant model terms (not counting those required to support hierarchy) can be removed and may result in an improved model. By selecting the backward elimination procedure to automatically reduce the terms that are not significant, the resulting ANOVA table for the reduced quadratic model for adsorption of Cu(II) is shown in Table 5.

The Model *F*-value of 139.15 implies the model is significant. There is only a 0.41% chance that a "Model *F*-Value" this large could occur due to noise. However, the main effect of pH (A), concentration (B), and time (C), the two-level interactions of pH and concentration (AB), and pH and time (AC), square term pH^2 (A^2), and concentration^2 (B^2) are the significant model terms. The R^2 value is high (0.9908), close to 1, which is desirable. The "Pred. R-Squared" of 0.9517 is in reasonable agreement with the "Adj R-Squared" of 0.9837. The adjusted R^2 value is particularly useful when comparing models with different number of terms. "Adequate Precision" measures the signal-to-noise ratio which should be more than four and in our case, it comes around 38.494. So, this model can be used to navigate the design space.

4.4. *Response surface estimation for maximum removal of Cu(II)*

4.4.1. *Effect of pH and contact time*

Adsorption experiments are carried out as per the selected model with selected range of Cu(II) concentration to investigate the combined effect of pH and contact time on the % removal of Cu(II) and presented in 3D plot (Fig. 7).

From Fig. 7, it can be concluded that with an increase in contact time, removal efficiency is increased linearly. The graph also shows that the maximum adsorption (95.221%) occurs under alkaline conditions (pH 8.0) which is in accordance with the model. Increasing the solution pH from 2 to 8 increases the % removal of Cu(II) by HAp was observed first by Wu et al. [57] and mentioned the possible reactions responsible for surface properties of HAp in aqueous solutions (Eqs. (10) and (11)).

$$\mathrm{P-O^- + H^+ \rightleftarrows P-OH} \tag{10}$$

$$\mathrm{Ca-OH_2^+ - H^+ \rightleftarrows Ca-OH} \tag{11}$$

Fig. 7 indicates adsorption % of metal ions increased when initial pH is increased. The adsorption mainly begins pH 5 with linear increase up to pH 8. This can be explained on the basis of proton competitive sorption reaction. At low pH due to the presence of higher concentration of H^+ ions compete with Cu^{2+} ions for surface binding sites of adsorbent cause lower adsorption %. When pH is increased, then the amount of H^+ ions is decreased and metal ions can bind free binding sites. This may cause increase in adsorption capacity. At lower pH, the existing relatively high concentration of H^+ increases the positively charged $CaOH_2^+$ and neutral POH. As a result, the surface of the sorbent is positively charged. Increased net positive charge is

Table 5
ANOVA table for the reduced quadratic model for adsorption of Cu(II)

Source	Sum of squares	df	Mean square	*F*-value	*p*-value prob. > F	
Model	2,595.32	7	370.76	139.15	<0.0001	significant
A-PH	1,868.32	1	1868.32	701.21	<0.0001	
B-concentration	46.35	1	46.35	17.40	0.0024	
C-time	314.50	1	314.50	118.04	<0.0001	
AB	39.29	1	39.29	14.75	0.0040	
AC	62.14	1	62.14	23.32	0.0009	
A^2	238.96	1	238.96	89.68	<0.0001	
B^2	35.13	1	35.13	13.19	0.0055	
Residual	23.98	9	2.66			
Lack of fit	21.63	5	4.33	7.36	0.0380	
Pure error	2.35	4	0.59			
Cor total	2,619.30	16				
Std. dev.	1.63	R-squared	0.9908			
Mean	73.43	Adj R-squared	0.9837			
C.V. %	2.22	Pred R-squared	0.9517			
Press	126.40	Adeq precision	38.494			

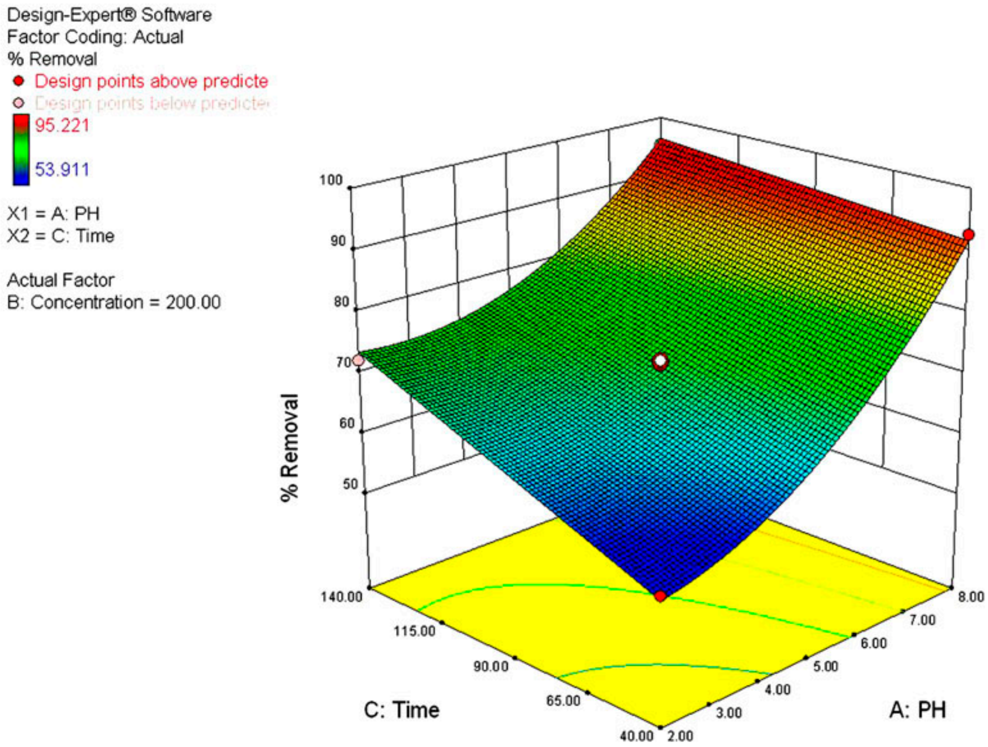

Fig. 7. 3D plot showing the effect of % removal of Cu(II) with pH and time.

less favorable in complexing Cu^{2+} on the sorbent surface than the net negative charge sites. Thus, increased net positive charge onto HAp surface in the pH range 2–3 may be attributed to decrement of Cu^{2+} removal. Precipitation plays a major role in removing metal ions in alkaline range. Above pH 6.5, precipitations of Cu^{2+} occur. The sorption process is kinetically faster than the precipitation and that is why the precipitation of metal hydroxide into the pores or spaces around the particles is hardly possible. [58,59]. Cu(II)

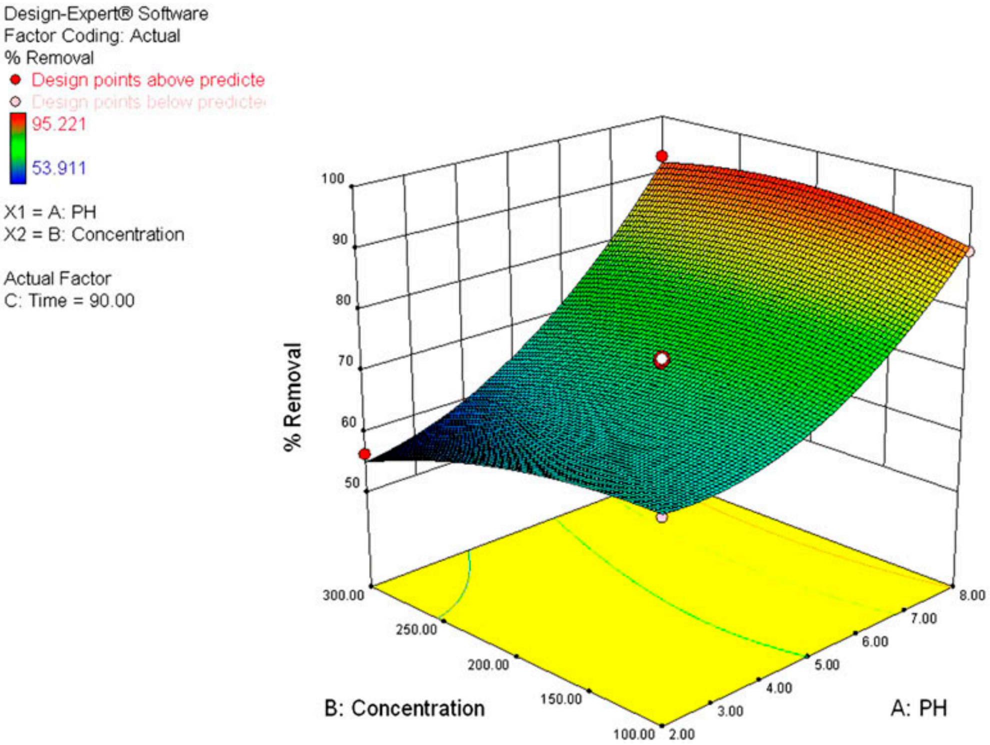

Fig. 8. 3D plot showing the effect of % removal of Cu(II) with pH and concentration.

Table 6
Optimization result

Sl. No.	PH	Concentration	Contact Time	% Removal	Desirability	
1	8.00	212.93	40.00	91.7707	0.957	Selected
2	8.00	214.11	40.00	91.7702	0.957	
3	8.00	219.25	40.00	91.758	0.957	
4	8.00	200.85	40.00	91.731	0.957	
5	8.00	224.52	40.00	91.7298	0.957	
6	8.00	211.32	40.12	91.7762	0.957	
7	8.00	194.08	40.00	91.6719	0.956	
8	8.00	217.60	40.29	91.7768	0.956	
9	8.00	233.84	40.00	91.6407	0.956	
10	8.00	206.44	40.38	91.7746	0.956	
11	8.00	235.67	40.00	91.6173	0.955	
12	8.00	187.45	40.00	91.5883	0.955	
13	8.00	236.96	40.10	91.6041	0.955	
14	7.98	222.71	40.00	91.5307	0.954	
15	8.00	183.10	40.00	91.5197	0.954	
16	8.00	243.46	40.00	91.4961	0.954	
17	7.97	195.35	40.00	91.3346	0.952	
18	8.00	168.76	40.00	91.2164	0.950	
19	8.00	256.94	40.00	91.2037	0.950	
20	8.00	258.13	40.00	91.1728	0.950	

removal by HAp adsorption is dominantly controlled between pH 5–8. The optimum Cu^{2+} removal by HAp is obtained at pH 8.

4.4.2. Effect of pH and Cu(II) concentration

Combined effect of pH and Cu(II) concentration has been analyzed from the Box–Behnken model as depicted in Fig. 8 and it has been estimated that as Cu (II) concentration increases from 100 to 200 mg/L, keeping time constant, the system and effect of metal ion concentration on the removal efficiency are also analyzed and it is found that results are in accordance with the suggested model given by RSM software. Increased adsorption up to 220 mg/L concentration may be attributed to the fact that higher initial concentration which causes an important driving force to overcome all mass transfer resistance of pollutant between the aqueous and solid phases thus increases the uptake. However, at 250–300 mg/L, a decline in copper adsorption is occurred. This decrease in Cu(II) adsorption at high concentration may be due to competition among metal ions for smaller number of available binding sites and also saturation of most of the binding sites.

4.4.3. Optimization of adsorption conditions

During optimization process, the aim was to find the optimal values of removal % in order to minimize the values of contact time during the adsorption process when pH and concentration are in range. Keeping this in mind, the optimal solutions are found out as pH 8.0, concentration 212.93 mg/L, and time 40 min with 95.70% desirability level and this is reported in Table 6.

Optimized effect of pH and Cu(II) concentration has been analyzed from the Box–Behnken model. To support the optimized data given by numerical modeling under optimized conditions, the confirmatory experiments are conducted with the parameters as suggested by the model and the percent removal is found to be 91.77%. The effects of pH and copper concentration are also studied to support the results and the data are in accordance with the results obtained from optimized conditions.

5. Conclusion

The study reveals that HAp powder synthesized from fish scale is a potential adsorbent for Cu(II) ion removal from aqueous solution. Pure crystalline HAp is obtained in a low-cost manner from fish scale waste utilization. Adsorption of Cu(II) onto HAp is described well by the pseudo-second-order kinetic model than pseudo-first-order kinetic model. Langmuir isotherm fitted experimental data with high correlation coefficient and maximum adsorption capacity is found to be 209.73 mg/g of Cu(II) on HAp. At lower pH range, adsorption is hindered mainly by the presence of H^+ ions. The Cu(II) adsorption onto HAp is very fast during initial sorption period. The optimal conditions for Cu(II) adsorption are found to be pH 8, contact time of 40 min, and metal concentration of 212.93 mg/L when 91.77% removal can be achieved using RSM approach with a desirability of 95.70%. The experimental results also are found to be in accordance with RSM results.

Acknowledgments

The authors would like to express their gratitude to the Director, CSIR-CMERI for his kind permission to publish this paper. The authors are also grateful to CSIR, Govt. of India, for the financial support through CLEAN WATER (ESC-0306) project. The help rendered by our scientific and technical staffs of CAMP, CSIR-CMERI, Durgapur, is highly acknowledged. The authors are also thankful to IIT, Kharagpur, for SEM and XRD analysis and Indian Association for the Cultivation of Science (IACS), Kolkata, for TEM work.

References

[1] J. Zolgharnein, N. Asanjarani, S. Norollah, Mousavi, optimization and characterization of Tl(I) adsorption onto modified *Ulmus carpinifolia* tree leaves, Clean–Soil, Air, Water 39(3) (2010) 250–258.

[2] M. Amini, H. Younesi, Biosorption of Cd(II), Ni(II) and Pb(II) from aqueous solution by dried biomass of *Aspergillus niger*: Application of response surface methodology to the optimization of process parameters, Clean–Soil, Air, Water 37(10) (2009) 776–786.

[3] M.R. Gandhi, G.N. Kousalya, S. Meenakshi, Removal of Cu(II) using chitin/chitosan nano-hydroxyapatite composite, Int. J. Biol. Macromol. 48 (2011) 119–124.

[4] N.R. Bishnoi, A.G. Pant, Biosorption of copper from aqueous solution using algal biomass, J. Sci. Ind. Res. 63 (2004) 813–816.

[5] D.C. Panadare, V.G. Lade, V.K. Rathod, Adsorptive removal of copper(II) from aqueous solution onto the waste sweet lime peels (SLP): Equilibrium, kinetics and thermodynamics studies, Desalin. Water Treat. 52 (40–42) (2014) 7822–7837.

[6] I. Villaescesa, N. Fiol, M. Martinez, N. Miralles, J. Poch, J. Serarols, Removal of copper and nickel ions from aqueous solutions by grape stalk wastes, Water Res. 38 (2004) 992–1002.

[7] A. Saeed, M. Iqbal, M.W. Akhtar, Removal and recovery of lead (II) from single and multimetal (Cd, Cu, Ni, Zn) solutions by crop milling waste (black gram husk), J. Hazard. Mater. 117 (2005) 65–73.

[8] M.T. Alslaibi, I. Abustan, M.A. Ahmadb, A.A. Foul, Kinetics and equilibrium adsorption of iron (II), lead (II), and copper(II) onto activated carbon prepared from olive stone waste, Desalin. Water Treat. 52 (40–42) (2014) 7887–7897.

[9] P. Salehi, F.M. Tajabadi, H. Younesi, Y. Dashti, Optimization of lead and nickel biosorption by *Cystoseira trinodis* (Brown algae) using response surface methodology, Clean–Soil, Air, Water 42(3) (2014) 243–250.

[10] M.R. Sangi, A. Shahmoradi, J. Zolgharnein, G.H. Azimi, M. Ghorbandoost, Removal and recovery of heavy metals from aqueous solution using *U. carpinifolia* and Fraxinus excelsior tree leaves, J. Hazard. Mater. 155 (2008) 513–522.

[11] A.J.M. Barros, S. Prasad, V.D. Leite, A.G. Souza, Biosorption of heavy metals in upflow sludge columns, Bioresour. Technol. 98 (2007) 1418–1425.

[12] L.S. Clesceri, A.E. Greenberg, A.D. Eaton, In Standard methods for the examination of water and waste water, twentieth ed., American Public Health Association, Washington, DC, 1998.

[13] M. Amini, H. Younesi, Biosorption of Cd(II), Ni(II) and Pb(II) from aqueous solution by dried biomass of Aspergillus niger: Application of response surface methodology to the optimization of process parameters, Clean–Soil, Air, Water 37(10) (2009) 776–786.

[14] E. Fourest, C. Canal, J.-C. Roux, Improvement of heavy metal biosorption by mycelial dead biomasses (*Rhizopus arrhizus*, *Mucor miehei* and *Penicillium chrysogenum*): pH control and cationic activation, FEMS Microbiol. Rev. 14(4) (1994) 325–332.

[15] B. Volesky, Z.R. Holan, Biosorption of heavy metals, Biotechnol. Prog. 11(3) (1995) 235–250.

[16] J.P. Chen, L. Hong, S. Wu, L. Wang, Elucidation of Interactions between metal ions and Ca alginate-based ion-exchange resin by spectroscopic analysis and modeling simulation, Langmuir. 18(24) (2002) 9413–9421.

[17] D. Das, N. Das, L. Mathew, Kinetics, equilibrium and thermodynamic studies on biosorption of Ag(I) from aqueous solution by macrofungus *Pleurotus platypus*, J. Hazard. Mater. 184 (2010) 765–774.

[18] J. Zolgharnein, T. Shariatmanesh, N. Asanjarani, *Cercis siliquastrum* tree leaves as an efficient adsorbent for removal of Ag(I): Response surface optimization and characterization of biosorption, Clean–Soil, Air, Water 41(12) (2013) 1183–1195.

[19] N. Das, Recovery of precious metals through biosorption-a review, Hydrometallurgy 103 (2010) 180–189.

[20] D. Sud, D. Mahajan, M.P. Kaur, Agricultural waste material as potential adsorbent for sequestering heavy metal ions from aqueous solutions—a review, Bioresour. Technol. 99 (2008) 6017–6027.

[21] B.I. Olu-Owalabi, E.I. Unuabonah, Kinetic and thermodynamics of the removal of Zn2\xFE and Cu2\xFE from aqueous solution by sulphate and phosphate-modified bentonite clay, J. Hazard. Mater. 184 (2010) 731–738.

[22] M. Sarkar, A.R. Sarkar, J.L. Goswami, Mathematical modeling for the evaluation of zinc removal efficiency on clay sorbent, J. Hazard. Mater. 149 (2007) 666–674.

[23] N. Chiron, R. Guilet, E. Deydier, Adsorption of Cu(II) and Pb(II) onto a grafted silica isotherms and kinetic models, Water Res. 37 (2003) 3079–3086.

[24] E.-S.Z. El-Ashtoukhy, N.K. Amin, O. Abdelwahab, Removal of lead(II) and copper(II) from aqueous solution using pomegranate peel as a new adsorbent, Desalination 223 (2008) 162–173.

[25] A.A. Bsoul, The use of eucalyptus leaves as adsorbent for copper ion removal, Desalin. Water Treat. 52 (40–42) (2014) 7838–7844.

[26] K.L. Dorrls, B. Yu, Y. Zhang, A. Shukla, S.S. Shukla, The removal of heavy metal from aqueous solutions by sawdust adsorption- removal of copper, J. Hazard. Mater. 80 (2000) 33–42.

[27] V.B.H. Dang, H.D. Doan, T. Dang-Vu, A. Lohi, Equilibrium and kinetics of biosorption of cadmium (II) and copper(II) Ions by wheat straw, Bioresour. Technol. 100 (2009) 211–219.

[28] N. Boujelben, J. Bouzid, Z. Elouear, Adsorption of nickel and copper onto natural iron oxide-coated sand from aqueous solutions: Study in single and binary systems, J. Hazard. Mater. 163(1) (2009) 376–382.

[29] C.A. Rozaini, K. Jain, C.W. Oo, K.W. Tan, L.S. Tan, A. Azraa, K.S. Tong, Optimization of nickel and copper ions removal by modified mangrove barks, Int. J. Chem. Eng. Appl. 1(1) (2010) 84–89.

[30] F. Güzel, H. Yakut, G. Topal, Determination of kinetic and equilibrium parameters of the batch adsorption of Mn(II), Co(II), Ni(II) and Cu(II) from aqueous solution by black carrot (*Daucus carota* L.) residues, J. Hazard. Mater. 153(3) (2008) 1275–1287.

[31] N. Ertugay, Y.K. Bayhan, The removal of copper(II) ion by using mushroom biomass (*Agaricus bisporus*) and kinetic modelling, Desalination 255 (2010) 137–142.

[32] M.V. Dinu, E.S. Dragan, Evaluation of Cu^{2+}, Co^{2+} and Ni^{2+} ions removal from aqueous solution using a novel chitosan/clinoptilolite composite: Kinetics and isotherms, Chem. Eng. J. 160 (2010) 157–163.

[33] A. Saeed, M.W. Akhter, M. Iqbal, Removal and recovery of heavy metals from aqueous solution using papaya wood as a new biosorbent, Sep. Purif. Technol. 45 (2005) 25–31.

[34] C.-S. Zhu, L.-P. Wang, W.-B. Chen, Removal of Cu(II) from aqueous solution by agricultural byproduct: Peanut hull, J. Hazard. Mater. 168 (2009) 739–746.

[35] X. Wang, Z.Z. Li, C. Sun, A comparative study of removal of Cu(II) from aqueous solutions by locally low-cost materials: Marine macroalgae and agricultural by product, Desalination 25 (2009) 146–159.

[36] Z. Aksu, İ.A. İşoğlu, Removal of copper(II) ions from aqueous solution by biosorption onto agricultural waste sugar beet pulp, Process Biochem. 40 (2005) 3031–3044.

[37] V. Espinosa, M.H. Esparza, F.A. Ruiz-Treviňo, Adsorptive properties of fish scales of *Oreochromis Niloticus* (*Mojarra Tilapia*) for metallic ion removal from waste water, Ind. Eng. Chem. Res. 40 (2001) 3563–3569.

[38] A. Chowdhury, A. Bhowal, S. Datta, Equilibrium, thermodynamic and kinetic studies for removal of copper(II) from aqueous solution by onion and garlic skin, Water 4 (2012) 37–51.

[39] M. Rafatullah, O. Sulaiman, R. Hashim, A. Ahmad, Adsorption of copper(II) onto different adsorbents, J. Dispersion Sci. Technol. 31 (2010) 918–930.

[40] B. Yu, Y. Zhang, A. Shukla, S.S. Shukla, K.L. Dorris, The removal of heavy metals from aqueous solutions by sawdust adsorption- removal of copper, J. Hazard. Mater. 80(1–3) (2000) 33–42.

[41] X. Chen, J. Wright, J.L. Conca, L.M. Peurrung, Effects of pH on heavy metal sorption on mineral apatite, Environ. Sci. Technol. 31 (1997) 624–631.

[42] U.K. Garg, M.P. Kaur, D. Sud, V.K. Garg, Removal of nickel (II) from aqueous solution by adsorption on agricultural waste biomass using a response surface methodological approach, Bioresour. Technol. 99 (2008) 1325–1331.

[43] A.S. Souza, W.N.L. dos Santos, S.L.C. Ferreira, Application of Box–Behnken design in the optimization of an on-line pre-concentration system using knotted reactor for cadmium determination by flame atomic absorption spectrometry, Spectrochim. Acta, Part B 60 (2005) 737–742.

[44] C.A. Toles, W.E. Marshall, M.M. Johns, GAC from nutshells for the uptake of metal ions and organic compounds, Carbon 35 (1997) 1414–1470.

[45] S. Mondal, R. Bardhan, B. Mondal, A. Dey, S.S. Mukhopadhyay, R. Guha, K. Roy, S. Roy, Synthesis characterization and *in vitro* cytotoxicity assessment of hydroxyapatite from different bio sources for tissue engineering application, Bull. Mater. Sci. 35(4) (2012) 683–691.

[46] S. Mondal, S. Mahata, S. Kundu, B. Mondal, Processing of natural resourced hydroxyapatite material from fish scale, Adv. Appl. Ceram. 109 (2010) 234–239.

[47] S. Mondal, A. Mondal, B. Mondal, N. Mandal, A. Dey, S.S. Mukhopadhyay, S. Singh, Physico-chemical characterization and biological response of *Labeo rohita*-derived hydroxyapatite scaffold, Bioprocess. Biosyst. Eng. 37(7) (2014) 1233–1240.

[48] M.M. Nassar, The kinetics of basic dye removal using palm fruit bunch, Adsorpt. Sci. Technol. 15 (1997) 609–617.

[49] Y.S. Ho, G. Mckay, Pseudo second order model for sorption process, Process Biochem. 34 (1999) 451–465.

[50] Y.S. Ho, D.A. Wase John. C.F. Forster, Study of the sorption of divalent metal ions onto peat. Adsorpt. Sci. Technol. 18 (2000) 639–650.

[51] S. Lu, S.W. Gibbs, Copper removal from wastewater using spent-grain as biosorbent, Bioresour. Technol. 99 (2008) 1509–1517.

[52] I. Langmuir, The adsorption of gases on plane surfaces of glass, mica and platinum, J. Am. Chem. Soc. 40 (1918) 1361–1365.

[53] S. Debnath, U.C. Ghosh, Kinetics, isotherm and thermodynamics for Cr(III) and Cr(VI) adsorption from aqueous solutions by crystalline hydrous titanium oxide, J. Chem. Thermodyn. 40 (2008) 67–77.

[54] İ. Özbay, U. Özdemir, B. Özbay, S. Veli, Kinetic, thermodynamic, and equilibrium studies for adsorption of azo reactive dye onto a novel waste adsorbent: Charcoal ash, Desalin. Water Treat. 51 (2013) 31–33.

[55] N.Gamze Turan, B. Mesci, O. Ozgonenel, Response surface modeling of Cu(II) removal from electroplating waste by adsorption: Application of Box–Behnken experimental design, Clean–Soil, Air, Water 41(3) (2013) 304–312.

[56] K. Tarangini, A. Kumar, G.R. Satpathy, V. Kumar Sangal, Statistical optimization of process parameters for Cr(VI) biosorption onto mixed cultures of *Pseudomonas aeruginosa* and *Bacillus subtilis*, Clean–Soil, Air, Water 37(4–5) (2009) 319 –627.

[57] L. Wu, W. Forsling, P. Schindler, Surface complexation of calcium minerals in aqueous solution: Surface protonation at fluorapatite—water interfaces, J. Colloid Interface Sci. 147 (1991) 178–185.

[58] F.M. Morel, J.G. Hering, Principles and applications of aquatic chemistry, Wiley, New York, NY, 1993.

[59] M. Madhava Rao, D.K. Ramana, K. Seshaiah, M.C. Wang, S.W. Chang Chien. Removal of some metal ions by activated carbon prepared from *Phaseolus aureus* hulls, J. Hazard. Mater. 166(2–3) (2009) 1006–1013.